Cancer Biol Med 2026. doi: 10.20892/j.issn.2095-3941.2025.0468

ORIGINAL ARTICLE

OPEN ACCESS

SARS-CoV-2 infection in brain tumors and the association with alterations in the tumor immune microenvironment

Weikang Chen[1,2*], Haojie Bai[2*], Maoling Tian[1*], Yanxia Huang[3*], Depei Li[1], Luyao Wu[1], Wei Li[2], Lei Zhou[2], Wange Lu[2], Xiaoxing Li[2], Linyi Liu[4], Xiaobing Jiang[1]

[1]Department of Neurosurgery, State Key Laboratory of Oncology in South China, Guangdong Provincial Clinical Research Center for Cancer, Sun Yat-sen University Cancer Center, Guangzhou 510060, China; [2]Institute of Precision Medicine, The First Affiliated Hospital, Sun Yat-sen University, Guangzhou 510000, China; [3]Department of Neurosurgery, The First Affiliated Hospital, Sun Yat-sen University, Guangzhou 510000, China; [4]Department of Neurosurgery, Northeast Yunnan Central Hospital, Zhaotong 657000, China

ABSTRACT

Objective: Recent clinical evidence indicates that persistent reservoirs of SARS-CoV-2 in human brain tissue are associated with various neurologic symptoms. While brain tumors have unique vascular abnormalities and immunosuppressive environments, it is unclear whether SARS-CoV-2 can infect brain tumors.

Methods: Brain tumor samples were collected from a cohort of 72 COVID-19 patients during the SARS-CoV-2 BA.5 wave in Guangzhou. SARS-CoV-2 infection was confirmed by quantitative reverse-transcription polymerase chain reaction (qRT-PCR) and immunohistochemical (IHC) staining. Immune cell infiltration within the tumor tissues was assessed using IHC. RNA-sequencing was performed to investigate virus-host interactions in the brain tumors.

Results: Brain tumor samples from 72 COVID-19 patients were examined and SARS-CoV-2 RNA was detected in 11% of the samples, which included samples from craniopharyngiomas, pituitary neuroendocrine tumors (PitNETs), meningiomas, and gliomas. SARS-CoV-2 infection was present in tumor and endothelial cells within these brain tumors. SARS-CoV-2-positive tumors had greater immune cell infiltration, particularly an increase in $CD8^+$ T cells in gliomas and pituitary PitNETs, along with the activation of innate signaling pathways. The transcriptomic analysis revealed that activation of the complement cascade within tumors may drive changes in the immune microenvironment of SARS-CoV-2-positive tumors.

Conclusions: These findings provided evidence of SARS-CoV-2 infection in brain tumors and suggested a role in altering the tumor immunosuppressive microenvironment.

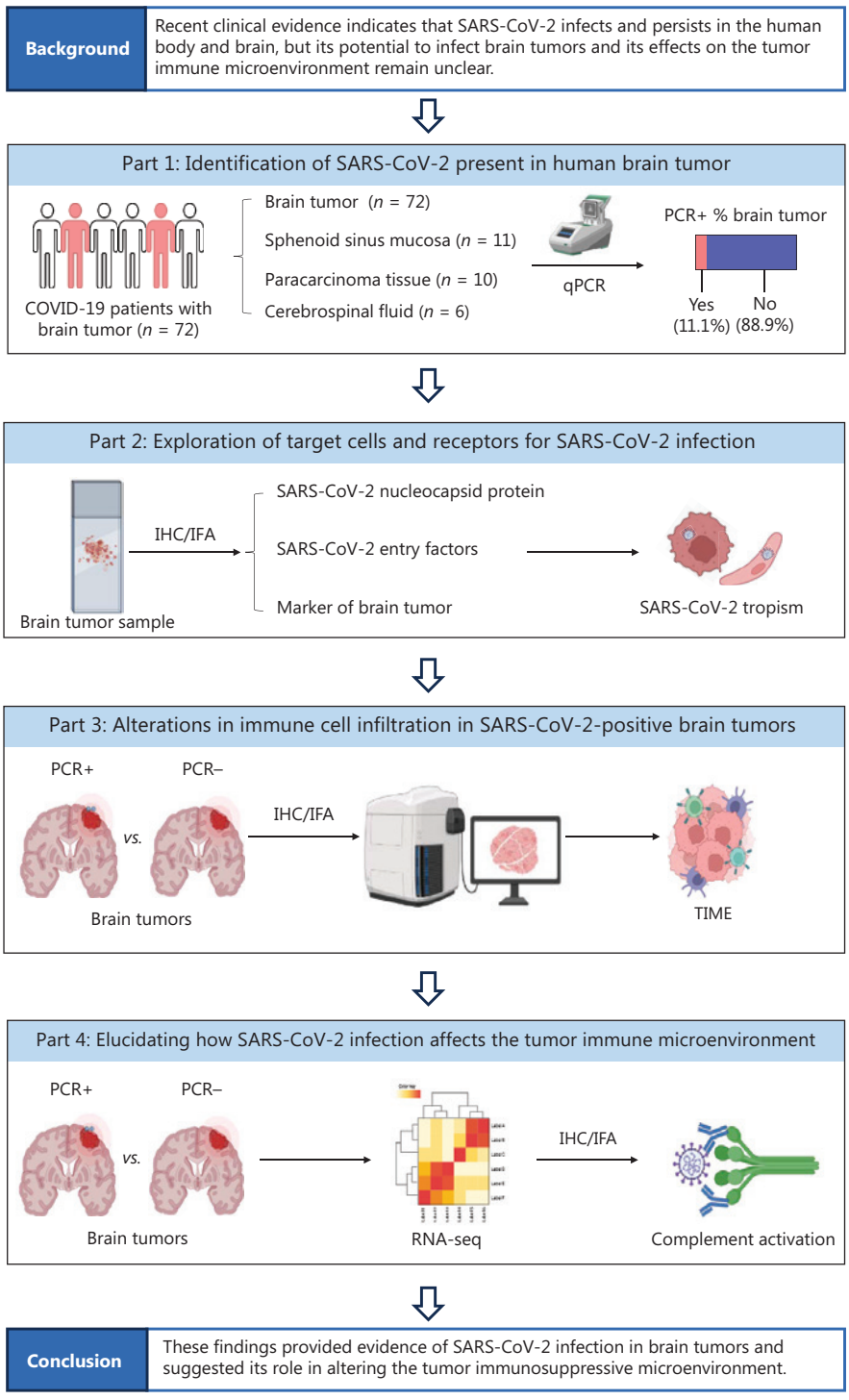
KEYWORDS SARS-CoV-2; brain tumors; immune microenvironment; innate immune; complement activation

Introduction

SARS-CoV-2 infection is associated with a wide range of neurologic complications, including headaches, encephalitis, cerebrovascular disorders, and long COVID syndrome, highlighting an ability to affect the central nervous system (CNS)[1-4]. Recent studies have detected SARS-CoV-2 RNA and proteins in brain tissue[5,6] with viral RNA and proteins detected in postmortem brain samples up to 7 months after initial infection[5]. The virus is hypothesized to access the central CNS through peripheral nerve pathways or the bloodstream, particularly in conditions in which the blood-brain barrier (BBB) is compromised, such as during brain tumor progression[6,7]. Brain tumors are characterized by an immunosuppressive microenvironment, which may create a favorable niche for viral persistence and replication[8,9]. However, SARS-CoV-2 infection in brain tumors and the effect on the tumor immune landscape remain poorly understood.

Tumors of the CNS are immunologically "cold" and exhibit limited infiltration of tumor-infiltrating lymphocytes (TILs) and various immune effector cells compared to peripheral tumors[10]. This immunosuppressive phenotype contributes to the poor response of brain tumors to immunotherapy, such as immune checkpoint blockade (ICB)[11]. Innate immune responses, particularly those involving the

*These authors contributed equally to this work.
Correspondence to: Xiaoxing Li, Linyi Liu and Xiaobing Jiang
E-mail: lixiaox23@mail.sysu.edu.cn, llysjwk1982@sina.com and jiangxiaob1@sysucc.org.cn
ORCID ID: https://orcid.org/0000-0001-8791-7505, https://orcid.org/0009-0006-1490-0685 and https://orcid.org/0000-0001-6566-7269
Received August 15, 2025; accepted January 6, 2026;
published online February 16, 2026.
Available at www.cancerbiomed.org
©2026 The Authors. Creative Commons Attribution-NonCommercial 4.0 International License (CC BY-NC 4.0)



Study flowchart

Part 1: During the SARS-CoV-2 BA.5 wave in Guangzhou, we collected 99 tissue samples from 72 COVID-19 patients with brain tumor. The samples included brain tumor tissues (*n* = 72), adjacent paracarcinoma tissues (*n* = 10), sphenoid sinus mucosa (*n* = 11), and cerebrospinal fluid (*n* = 6). The cohort included various brain tumors, comprising gliomas (*n* = 25, 34.7%), meningiomas (*n* = 19, 26.4%), and pituitary neuroendocrine tumors (*n* = 14, 19.4%). By conducting RT-qPCR, we examined SARS-CoV-2 RNA specifically targeting the viral N and ORF1ab genes in all 99 tissue samples.

Part 2: To identify target cells and receptors for SARS-CoV-2 infection in brain tumor samples, including pituitary neuroendocrine tumors, meningiomas, gliomas, and craniopharyngiomas, we used specific markers for malignant cells found in different brain tumors: TTF1 for PitNETs, MUC1 for meningiomas, GFAP for gliomas, and CK7 for craniopharyngiomas.

Part 3: To investigate the effects of SARS-CoV-2 on the TIME, we compared immune cell infiltration patterns between SARS-CoV-2 PCR-positive and PCR-negative brain tumors using IHC for specific immune cell subset markers.

Part 4: To comprehensively characterize the molecular alterations associated with the persistence of SARS-CoV-2 in brain tumors in an unbiased and comprehensive manner, we conducted transcriptome sequencing on a diverse set of brain tumor samples, including six pituitary neuroendocrine tumor samples, three glioma samples, two craniopharyngioma samples, and five meningioma samples.

CK7, cytokeratin 7; GFAP, glial frillary acidic protein; IFA, immunofluorescence assay; IHC, immunohistochemistry; MUC1, Mucin 1; N gene, nucleocapsid; ORF1ab gene, open reading frame 1ab; PitNETs, pituitary neuroendocrine tumors; qPCR, quantitative polymerase chain reaction; RT-qPCR, reverse transcription quantitative PCR; TIME, tumor immune microenvironment; TTF1, thyroid transcription factor 1.

complement system, have dual roles in antiviral defense and immune regulation in the tumor microenvironment[12]. Recent studies have implicated hyperactivation of the complement cascade in the pathogenesis of COVID-19[13,14], suggesting a link between viral infection and dysregulated immune responses. In addition, innate immune responses, including activation of the complement system, have immunoregulatory functions that remodel the tumor immune microenvironment (TIME), potentially influencing tumor progression[15,16].

In the current study, the presence of SARS-CoV-2 was investigated in brain tumors from a cohort of 72 COVID-19 patients. Viral RNA was detected in 11% of the tumor samples, including craniopharyngiomas, pituitary neuroendocrine tumors (PitNETs), meningiomas, and gliomas. By conducting a comprehensive analysis of immune infiltration patterns and molecular profiles, SARS-CoV-2 persistence in brain tumors was shown to be associated with alterations in the immune microenvironment, particularly *via* the complement system, reshaping the TIME. These findings provide new insights into the interaction between viral infection and the brain TIME with potential implications for therapeutic strategies involving the immunomodulatory function of SARS-CoV-2.

Materials and methods

Patients and samples

A total of 99 tissue samples from 72 patients diagnosed with brain tumors were collected from January to March 2023 during the SARS-CoV-2 BA.5 wave in Guangzhou, all of whom were diagnosed with COVID-19. The Ethics Committee of Sun Yat-sen University Cancer Center granted approval for the collection and use of human brain samples for this study (approval number B2020-165-01). Informed consent was obtained from all participants.

RNA extraction and SARS-CoV-2 RNA quantification

Samples were gathered and processed using the RNeasy Mini kit (74106; Qiagen, Hilden, Germany). The Detection Kit for 2019 Novel Coronavirus RNA (DA0932; DAAN, Guangzhou, China) was used to identify and measure SARS-CoV-2 RNA following the manufacturer's instructions. SARS-CoV-2 RNA was detected by RT-qPCR targeting the viral *N* and *ORF1ab* genes with no-template and positive controls included in each run to ensure assay quality. Samples were considered SARS-CoV-2-positive based on the manufacturer's criteria if a distinct amplification curve was generated with a CT value ≤ 40 for *N/ORF1ab* genes.

Antibodies and reagents

The following antibodies were used in the current study: anti-SARS-CoV-2-NP (40143-MM05, 1:100; Sino Biological, Beijing, china); anti-NRP1 (60067-1-Ig, 1:200; Proteintech, Rsemont, IL, USA); rabbit anti-CD31 (77699S, 1:500; Cell Signaling Technology, Danvers, MA, USA); rabbit anti-ACE2 (10108-T24, 1:200; Sino Biological); rabbit anti-TMPRSS2 (14437-1-AP, 1:200; Proteintech); mouse anti-CD147/BSG (66443-1-Ig, 1:200; Proteintech); anti-CD3 (85061s, 1:300; CST, Danvers, MA, USA); anti-CD4 (ab133616, 1:1000; Abcam, Cambridge, United Kingdom); anti-CD8 (ab93278, 1:200; Abcam); anti-CD8 (66868-1-Ig, 1:200; Proteintech); anti-CD20 (ab9475, 1:1000; Abcam); anti-CD68 (76437s, 1:500; CST); anti-C3 (ET7106-75, 1:100; Huabio, Fort Worth, TX, USA); anti-C1q (HA721439, 1:100; Huabio); anti-IgG (ZA-0448; ZSGB-BIO, Beijing, China); anti-IgM (ZA-0450; ZSGB-BIO); anti-TTF1 (66034-1-Ig, 1:200; Proteintech); rabbit anti-GFAP (16825-1-AP, 1:200; Proteintech); anti-MUC1 (HA601142, 1:200; Huabio); anti-panCK (HA601138, 1:200; Huabio); anti-PD-1 (18106-1-AP, 1:200; Proteintech); anti-IFN-γ (AB231036, 1:200; Abcam); and anti-FOXP3 (22228-1-AP, 1:200; Proteintech).

Hematoxylin and eosin (H&E) staining

Tissue samples from patients were fixed in 4% paraformaldehyde, embedded in paraffin, and cut into 4-μm sections. The slides were heated at 65°C for 2 h, then deparaffinized using xylene, rehydrated, and washed with water. The sections were subsequently stained with hematoxylin and eosin, dehydrated, cleared with xylene, and mounted using Mounting Medium (ZLI-9516; ZSGB-BIO). The slides were scanned with a KFbio scanner (KF-PRO-020; Zhejiang, China).

Immunohistochemistry (IHC) and immunofluorescence assay (IFA)

Brain tissue sections were deparaffinized, rehydrated, and underwent antigen retrieval in a pressure cooker at 120°C for 2 min using Tris-EDTA (pH 9.0) for IHC. Endogenous peroxidase activity was inhibited with 3% hydrogen peroxide. After blocking with 20% goat serum for 30 min brain tissue sections were incubated overnight at 4°C with primary antibodies, washed, then treated with secondary antibodies.

Brain tissue sections were blocked with 10% normal goat serum [NGS] (Solarbio, Beijing, China) in phosphate-buffered saline with Tween 20 [PBST] (TargetMol, Boston, MA, USA) at room temperature for 1 h, followed by incubation with primary antibodies diluted in 1% NGS for IFA. After an overnight incubation of the primary antibodies at 4°C the sections were washed 3 times with PBST, then stained with

the appropriate secondary antibodies in PBS at room temperature for 1.5 h. IFA was performed using a Branch TSA 4-color combination kit (TissueGnostics, Vienna, Austria) according to the manufacturer's instructions as previous procedure when primary antibodies originated from the same host[17]. After washing the sections were stained with DAPI (Solarbio). Finally, after washing with PBST the sections were mounted using Mounting Medium (ZSGB-BIO, China).

Quantification of CD68-, CD3-, CD4-, CD8-, CD20-, C1q-, C3-, IgG-, and IgM-positive cells was performed using QuPath software (version 0.3.2; Queen's University, Belfast, Northern Ireland). Between 5 and 8 randomly selected fields of view per sample were analyzed to maximize data yield from the limited positive samples available for each brain tumor type. Positive cells were manually counted within each field (area per field: 0.2 mm^2). The results are expressed as the average number of positive cells per square millimeter (cells/mm^2). All quantitative analyses were performed independently by two researchers blinded to the sample groupings. The final value for each sample represents the mean of the scores from two observers.

Bulk RNA sequencing and data analysis

Total RNA was isolated from SARS-CoV-2-positive or -negative brain tumors using TRIzol (Invitrogen, Carlsbad, CA, USA) and subjected to RNA sequencing by LC-BIO Bio-tech Ltd. (Hangzhou, China). RNA concentration and quality were assessed using a Nanodrop 2000 (Thermo Fisher Scientific, Waltham, MA, USA). An mRNA Purification Kit (Invitrogen) was utilized to remove rRNA and extract poly(A)$^+$ RNA using oligo d(T). The extracted mRNA was subsequently fragmented and short fragments were primed with random hexamers for the synthesis of first- and second-strand cDNA. Adenine (A) was added to the 3′ ends of the blunt fragments and indices and adapters were ligated during the adapter ligation and amplification process. The libraries were sequenced on an Illumina Hiseq 4,000 platform (Illumina, San Diego, CA, USA), producing 150-bp paired-end reads.

RNA-seq reads were aligned to the human reference genome (hg19) using HISAT2 (v2.1.0; https://github.com/DaehwanKimLab/hisat2) with default parameters. Transcript-level read counts were generated with htseq-count (v0.11.2; source). For differential expression analysis, Raw counts were imported into DESeq2 (v1.28.1) in RStudio (https://posit.co/download/rstudio-desktop/). Normalization was performed internally by DESeq2 using the median-of-ratios method. Differential gene expression was defined as a P value (<0.05) and fold-change (>2). The volcano map of the differentially expressed genes was produced by the R package, ggplot2 (v3.3.0). Functional enrichment analysis of Gene Ontology (GO) terms and Kyoto Encyclopedia of Genes and Genomes (KEGG) pathways was performed with the clusterProfiler R package. All services were provided by LC Biotech Corporation (Hangzhou, China).

Statistical analysis

Statistics were performed using GraphPad Prism 9 software (GraphPad Software, San Diego, CA, USA). The results were represented as the mean ± standard deviation (SD). The Mann–Whitney U test was used for all comparisons between two independent groups. An adjusted $P < 0.05$ was considered statistically significant.

Results

SARS-CoV-2 RNA is present in the brain tumor tissues of COVID-19 patients

Ninety-nine tissue samples were collected from 72 patients diagnosed with brain tumors from January to March 2023 during the SARS-CoV-2 BA.5 wave in Guangzhou, all of whom were also diagnosed with COVID-19 (**Figure 1A**). A total of 48.6% of these patients were male with a median age of 46.5 years [interquartile range (IQR): 36.5–59 years; clinical information in **Table S1**]. The samples included brain tumor tissues, adjacent paracarcinoma tissues, sphenoid sinus mucosae, and cerebrospinal fluids. The cohort included various brain tumors, comprised of gliomas [n = 25 (34.7%)], meningiomas [n = 19 (26.4%)], and PitNETs [n = 14 (19.4%); **Figure 1B**]. SARS-CoV-2 RNA specifically targeting the viral *N* and *ORF1ab* genes was examined in all 99 tissue samples by performing reverse transcription quantitative PCR (RT-qPCR). Viral *N* or *ORF1ab* RNA was identified in the sphenoid sinus mucosae [6/11 (55%)], brain tumor tissues [8/72 (11%)], and cerebrospinal fluids [1/6 (17%)] but not in paracarcinoma tissues (**Figure 1C and D**). Further analysis revealed SARS-CoV-2 RNA in 1 of 2 craniopharyngiomas (50%), 3 of 14 PitNETs (21%), 2 of 19 meningiomas (11%), and 2 of 25 gliomas (8%; **Figure 1E and F**). These findings suggested that SARS-CoV-2 infects human brain tumor tissues.

SARS-CoV-2 protein is expressed in human brain tumor tissues

IHC was performed to detect the SARS-CoV-2 nucleocapsid (N) protein in brain tumor samples. The viral N protein was detected in SARS-CoV-2 PCR-positive sphenoid sinus mucosae and various types of brain tumors, including PitNETs, meningiomas, gliomas, and craniopharyngiomas (**Figures 2A, B** and **S1**). However, due to low viral loads, some brain tumor tissues had no detectable viral protein expression. SARS-CoV-2 entry factor expression, including the classical receptor, ACE2, and the co-receptor, TMPRSS2, was analyzed with alternative receptors (CD147 and NRP1) to determine the

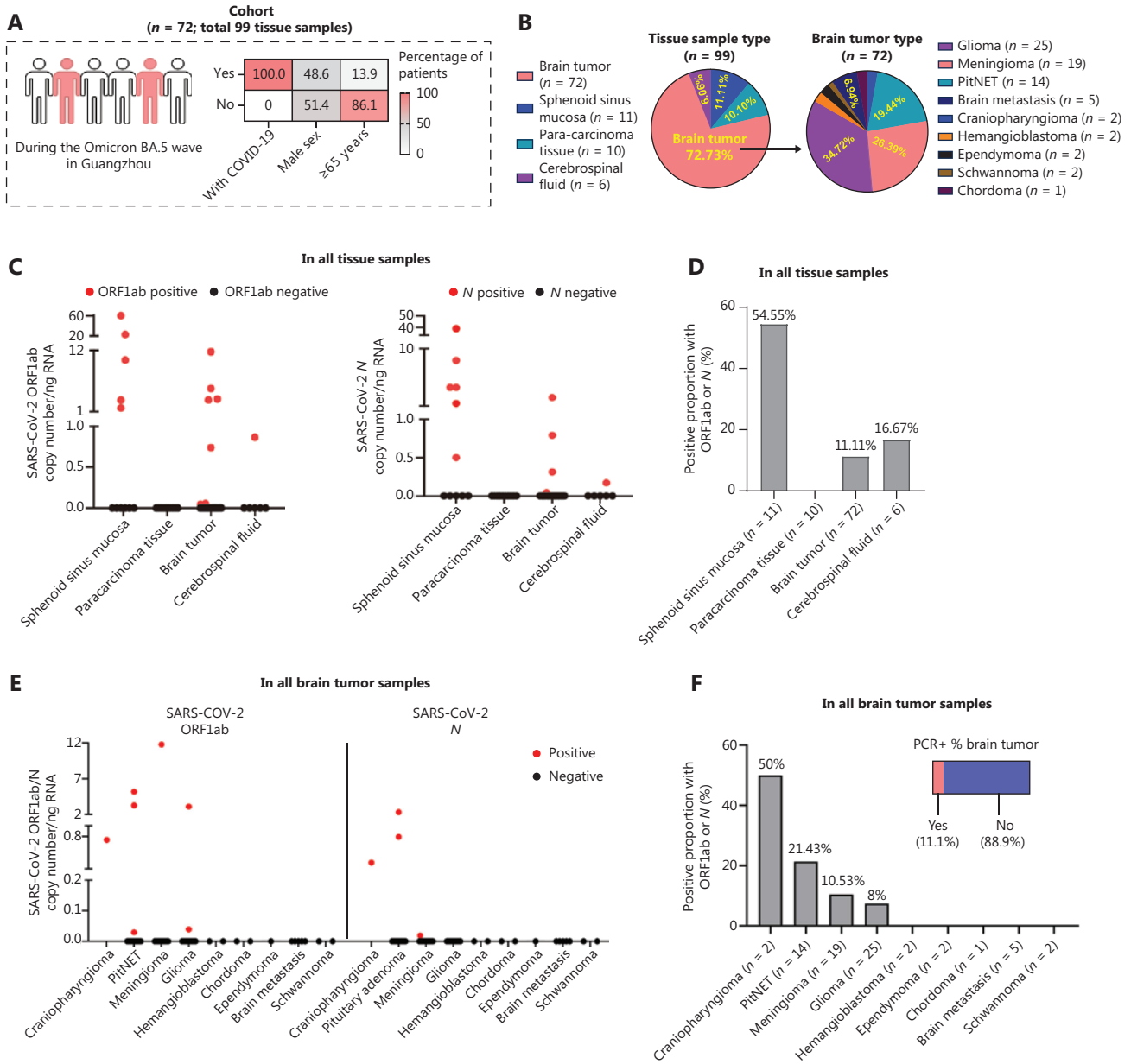


Figure 1 Presence of SARS-CoV-2 RNA in the brain tumor tissues of COVID-19 patients. (A) Overview of the study cohort, which included 72 brain tumor patients from Guangzhou during the Omicron BA.5 surge; details on COVID-19-positivity, age, and gender are provided. (B) Categorization of tissue samples, including various brain tumor types, such as gliomas, meningiomas, and pituitary neuroendocrine tumors (PitNETs), as well as non-brain tumor tissues, such as sphenoid sinus mucosae, paracancerous tissues, and cerebrospinal fluids. (C) Detection of SARS-CoV-2 RNA using the *ORF1ab* and *N* genes across all tissue samples. (D) Proportion of positive detection for the *ORF1ab* and *N* genes in all tissue samples. (E) Detection of SARS-CoV-2 RNA *via* the *ORF1ab* and *N* genes in different brain tumor subtypes. (F) Proportion of *ORF1ab* and *N* genes detected in various brain tumor subtypes.

mechanisms underlying viral entry into brain tumor tissues. IFA analysis revealed that ACE2 and TMPRSS2 expression is absent in brain tumors but NRP1 and CD147 expression is strong (**Figures 2C and S2**). These findings suggested that SARS-CoV-2 may directly infect brain tumor cells.

Specific markers for malignant cells found in different brain tumors were used to determine the ability of SARS-CoV-2 to infect tumor cells: TTF1 for PitNETs; MUC1 for meningiomas; GFAP for gliomas; and CK7 for craniopharyngiomas. These markers were then co-stained with viral nucleoprotein (NP).

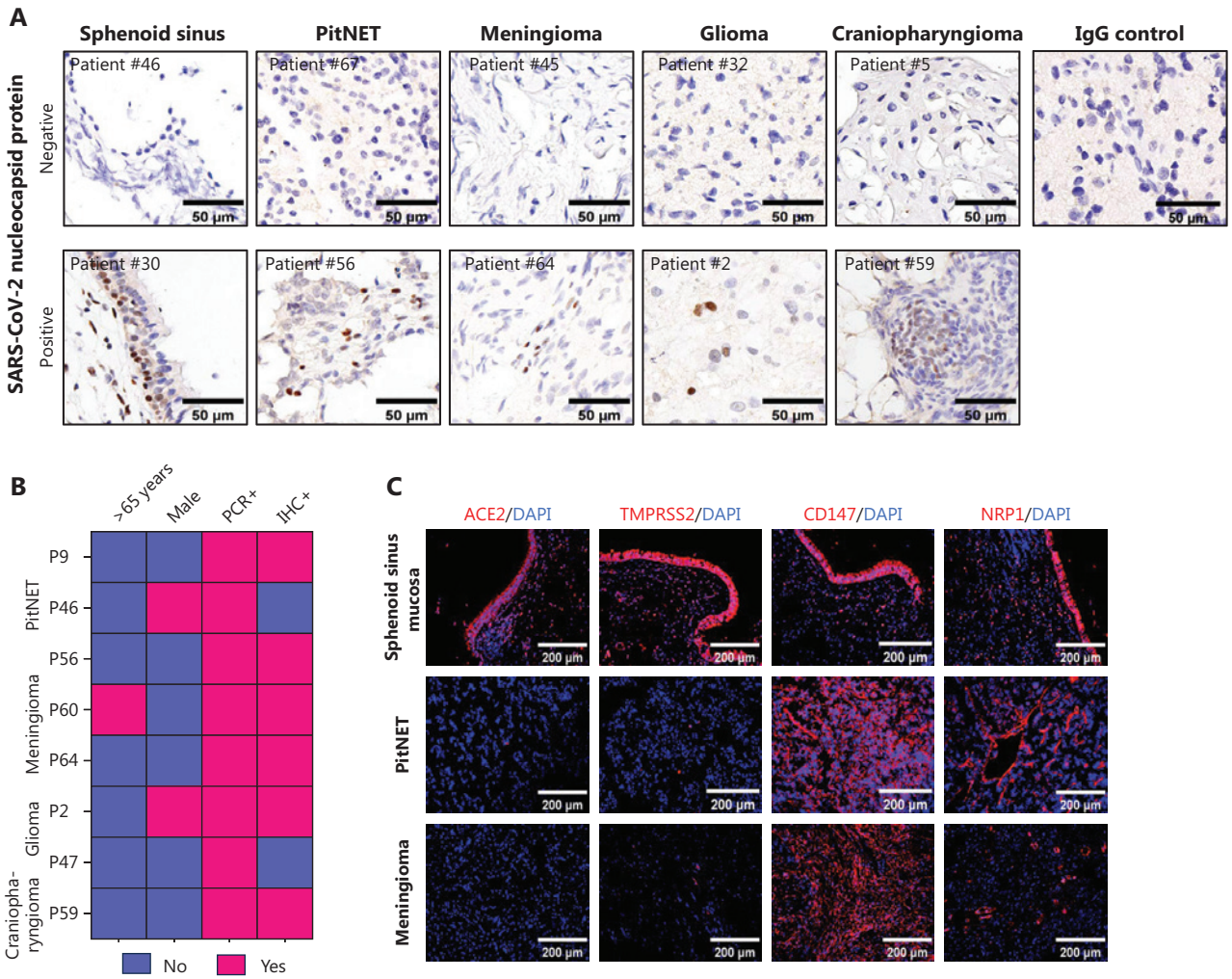


Figure 2 SARS-CoV-2 protein detection in human brain tumor tissue. (A) Representative IHC images of SARS-CoV-2 nucleocapsid protein in different brain tissue types that were SARS-CoV-2 PCR-negative or -positive; scale bars: 50 μm. (B) Patient characteristics, including age (>65 years), male gender, PCR-positivity, and IHC-positivity, for different brain tumor types. (C) Representative immunofluorescence images of SARS-CoV-2-related receptors, including ACE2, TMPRSS2, CD147, and NRP1, in different brain tissue types. Nuclei are stained with DAPI. Scale bars: 200 μm.

The results revealed that the viral NP protein is expressed in tumor cells from different brain tumors (**Figure 3A**). In addition, brain endothelial cells were permissive to SARS-CoV-2 infection (**Figure 3B**). These findings suggested that SARS-CoV-2 infects both tumor cells and endothelial cells in CNS tumors.

Alterations in immune cell infiltration in SARS-CoV-2-positive brain tumors

Immune cell infiltration patterns were compared between SARS-CoV-2 PCR-positive and -negative brain tumors using IHC for specific immune cell subset markers to determine the effects of SARS-CoV-2 on the TIME. SARS-CoV-2-positive and -negative brain tumors exhibited significant macrophage infiltration, as indicated by CD68 immunostaining. Infiltrating macrophages were the predominant immune cell type inside the intratumor inflammatory infiltrate, especially in meningiomas (**Figure 4A-H**). SARS-CoV-2-positive brain tumor patients presented a significantly greater density of $CD68^+$ macrophages than the negative counterparts (**Figure 4A-H**). A greater infiltration of $CD3^+$ T cells was demonstrated in SARS-CoV-2-positive PitNET and glioma patients than SARS-CoV-2-negative patients (**Figure 4A-D**). This trend was not evident in craniopharyngioma or meningioma patients (**Figure 4E-H**). Further analysis of T-cell subtypes revealed that $CD8^+$ T cells were more abundant than $CD4^+$ T cells across the intratumor zone, except for craniopharyngiomas (**Figure**

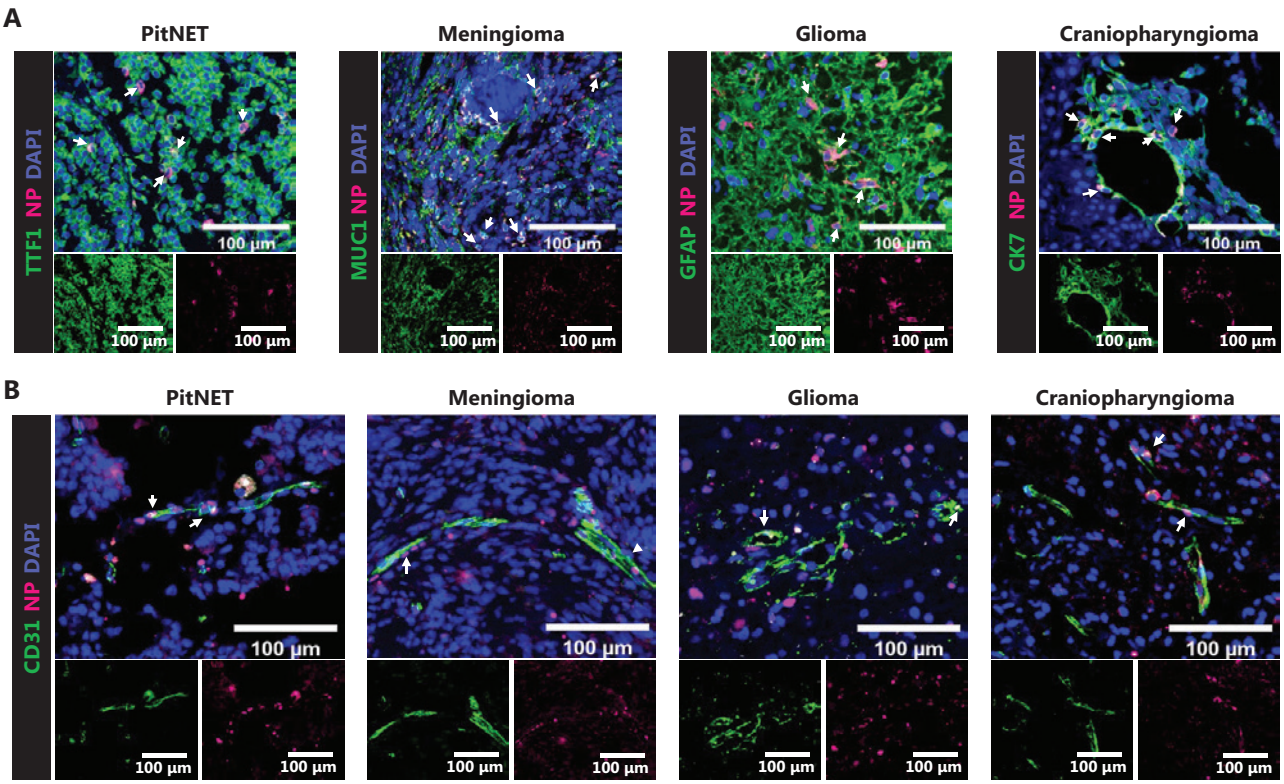


Figure 3 SARS-CoV-2 infection in brain tumor tissue. (A) Immunofluorescence co-staining of tumor markers (green) and nucleocapsid protein (red) in different brain tumor samples. Nuclei are stained with DAPI (blue). Scale bars: 100 μm. (B) Immunofluorescence co-staining of CD31 (green) and nucleocapsid protein (red) in different brain tumor samples. Nuclei are stained with DAPI (blue). Scale bars: 100 μm.

4A-H). Specifically, $CD8^+$ T-cell infiltration was more abundant in SARS-CoV-2-positive PitNET and glioma patients than SARS-CoV-2-negative patients (**Figure 4A and C**). Only a few $CD20^+$ B cells were sparsely distributed across all types of brain tumors and SARS-CoV-2 infection did not significantly alter B-cell infiltration in any of the four types of brain tumors examined (**Figure 4A-D**).

IFA staining analysis was performed with functional markers for $CD8^+$ (IFN-γ and PD-1) and $CD4^+$ T cells (FOXP3) to determine the immune phenotype of T cells (effector, exhausted, or regulatory). The density of effector $CD8^+$ T cells (IFN-γ^+ $CD8^+$ T cells) was significantly higher in SARS-CoV-2-positive brain tumors than -negative brain tumors (**Figure S3A**). In contrast, the density of exhausted $CD8^+$ T cells (PD-1^+ $CD8^+$ T cells) was significantly lower in positive tumors, except craniopharyngiomas (**Figure S3B**). However, the density of regulatory $CD4^+$ T cells ($FOXP3^+$ $CD4^+$ T cells) did not differ significantly between the two groups (**Figure S3C**). These findings indicated that the infiltrating $CD8^+$ T cells in SARS-CoV-2-positive brain tumors are predominantly of an effector phenotype. Moreover, correlation analysis was performed between viral copy number and intratumoral immune cell infiltration density. The viral load was associated with $CD8^+$ T cell infiltration but no correlation existed with $CD68^+$ macrophages, $CD3^+$ T cells, or $CD4^+$ T cell infiltration (**Figure 4I**). These findings suggested that SARS-CoV-2 infection is associated with alterations in the immune microenvironment of brain tumors.

Activation of intratumor innate immune signaling in SARS-CoV-2-positive brain tumors

Transcriptome sequencing was performed on a diverse set of brain tumor samples to characterize the molecular alterations associated with the persistence of SARS-CoV-2 in brain tumors in an unbiased and comprehensive manner, including six PitNET, three glioma, two craniopharyngioma, and five meningioma samples. GO and KEGG enrichment analyses revealed that significant upregulation of genes involved in pituitary hormone metabolism in SARS-CoV-2-positive PitNETs, revealing the potential effect of SARS-CoV-2 infection on the physiologic functions of PitNETs (**Figures 5A** and **S4A**). SARS-CoV-2-positive gliomas exhibited upregulation of antibacterial and antiviral immune responses with suppression of multiple metabolism-related pathways (**Figures 5B and S4B**).

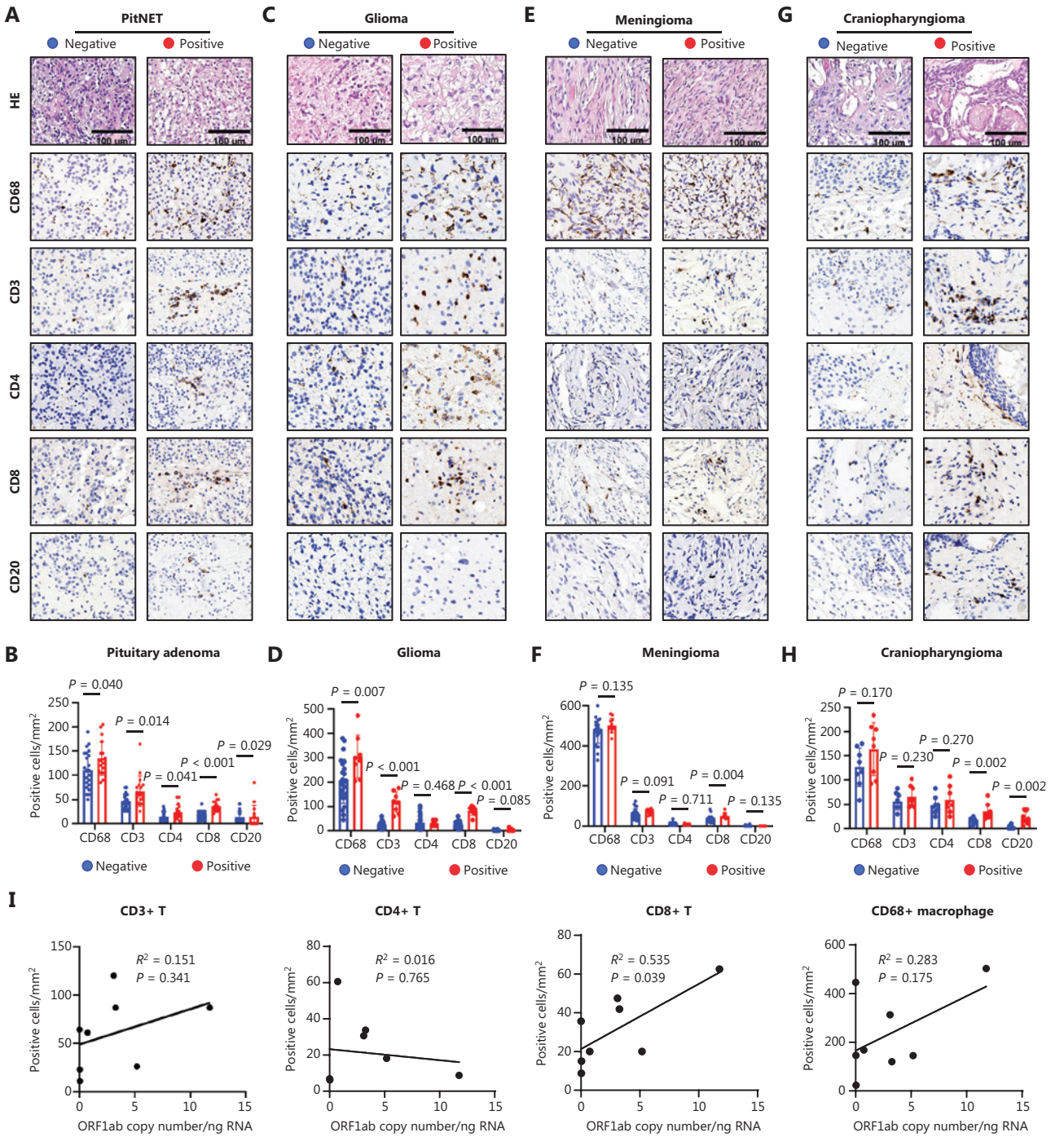


Figure 4 Alterations in immune cell infiltration in SARS-CoV-2-positive brain tumors. (A, C, E, and G) Representative images of H&E staining and immunohistochemical analysis of immune cell markers (CD68, CD3, CD4, CD8, and CD20) in SARS-CoV-2 PCR-negative and -positive brain tumors, including (A) pituitary neuroendocrine tumors, (C) gliomas, (E) meningiomas, and (G) craniopharyngiomas. Scale bars: 100 μm. (B, D, F, and H) Quantitative analysis of the density of positive immune cells (cells/mm^2) for each marker in (B) pituitary neuroendocrine tumors, (D) gliomas, (F) meningiomas, and (H) craniopharyngiomas; 5–8 fields/sample were analyzed. (I) Spearman's test shows a correlation between viral load and the degree of immune cell infiltration. The data represent the mean ± SD; statistical significance was determined by performing the Mann–Whitney *U* test and the adjusted *P* values are reported for multiple testing.

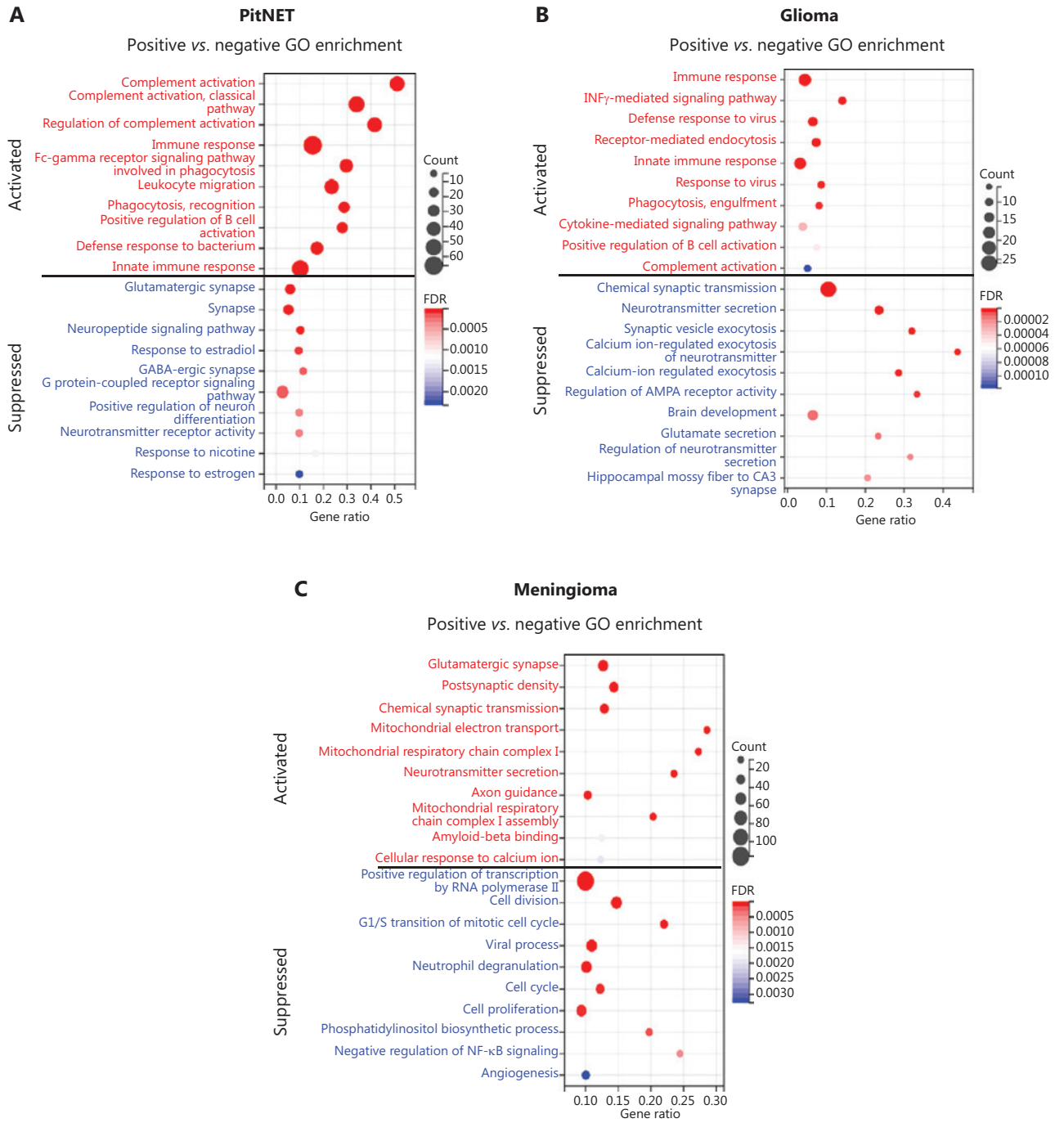


Figure 5 Continued

SARS-CoV-2-positive meningiomas exhibited upregulation in pathways related to neurodegeneration, mitochondrial OXPHOS, and calcium signaling but downregulation in viral response, cell cycle, and oncogenic pathways (**Figures 5C and S4C**). In addition, a significant reduction was noted in the expression of zinc finger protein-related genes, such as *ZNF177*, *ZNF140*, and *ZBTB11*, in SARS-CoV-2-positive meningiomas (**Figure S4D**). These genes are essential for protection against SARS-CoV-2 infection and the downregulation may weaken the tumor response to SARS-CoV-2 infection. Several oncogenic signaling pathways were downregulated in SARS-CoV-2-positive craniopharyngiomas, whereas multiple

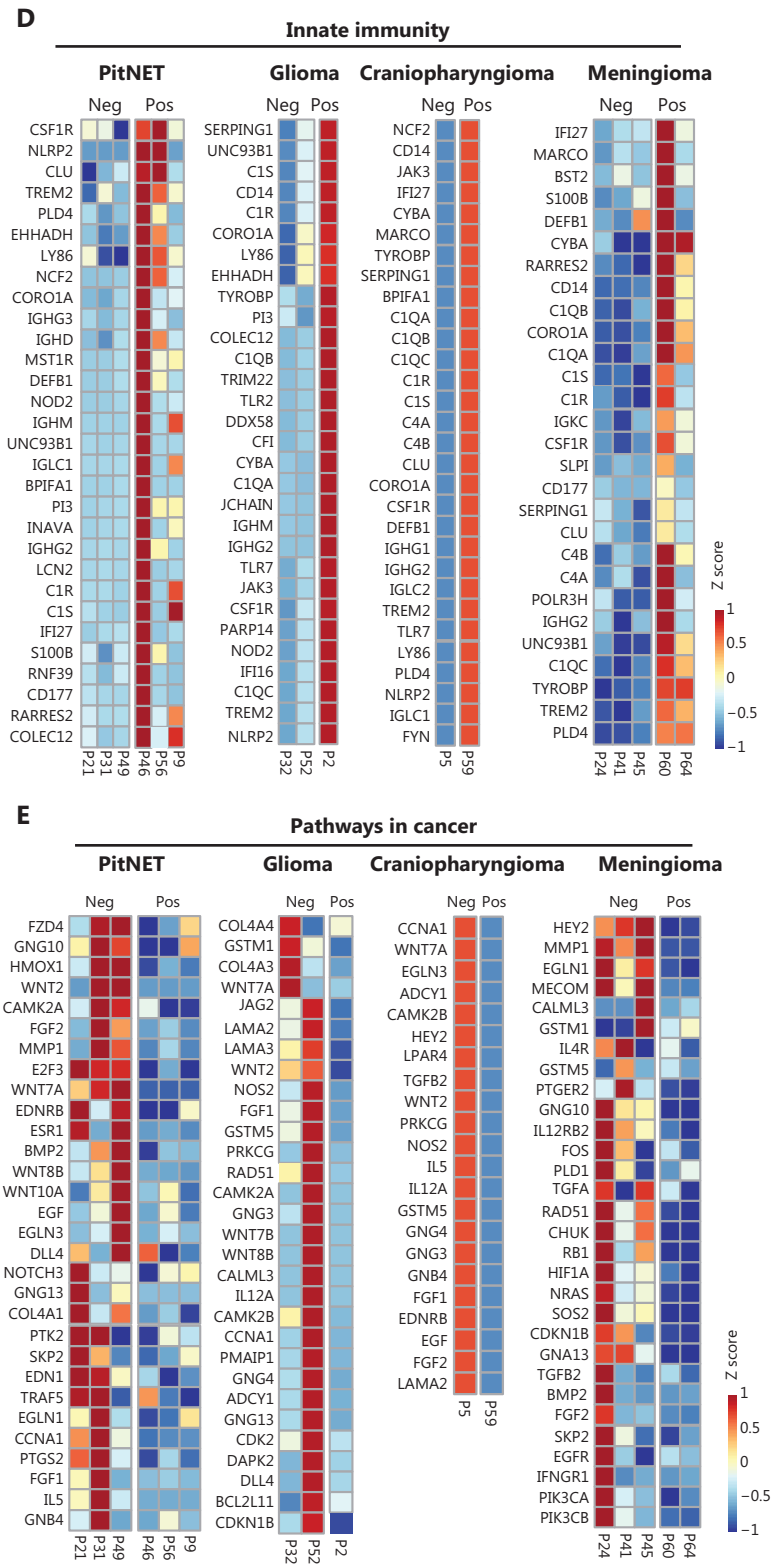


Figure 5 Activating innate immune signals in SARS-CoV-2-positive brain tumors. (A–C) Gene Ontology (GO) enrichment analysis comparing gene expression profiles between SARS-CoV-2 PCR-positive (Pos) and -negative (Neg) brain tumor samples. The differentially expressed genes and the corresponding GO terms for biological processes are illustrated for (A) pituitary neuroendocrine tumors, (B) gliomas, and (C) meningiomas. (D and E) Heatmaps of gene expression profiles involved in (D) innate immune signaling and (E) cancer-related pathways across SARS-CoV-2-positive and -negative brain tumor subtypes. The Z-scores represent normalized gene expression.

immune responses, including complement activation, inflammatory cytokine signaling, and IFN-γ signaling, were markedly activated (**Figure S4E and F**).

Multiple innate immune responses, including complement activation, phagocytosis, and antiviral responses, were upregulated in SARS-CoV-2-positive tumors based on a comprehensive analysis of SARS-CoV-2-positive tumors, whereas neural signal transmission and oncogenic pathways were reduced (**Figures 5A-C and S4A-D**). In addition, significant upregulation existed in complement- and antiviral response-related gene expression (e.g., *CSF1R*, *C1R*, *C1S*, *C1QB* and *IFI27*) in SARS-CoV-2-positive tumors (**Figure 5D**). Altered expression of key genes within oncogenic signaling pathways, such as *WNT*, *JAG2*, *WNT7A*, and *HEY2*, was also noted (**Figure 5E**). These results suggested that infection with SARS-CoV-2 in brain tumors is associated with activation of innate immune responses, while simultaneously suppressing pro-tumorigenic signaling pathways, highlighting the complex interaction between viral persistence and tumor biology.

SARS-CoV-2-positive tumors exhibit significant activation of the complement cascade

Gene set enrichment analysis (GSEA) was performed to identify the common pathways activated in SARS-CoV-2-infected brain tumors *versus* uninfected controls to elucidate the mechanism by which SARS-CoV-2 infection affects the TIME. The analysis revealed significant activation of the complement system in SARS-CoV-2-positive tumors across all types of brain tumors (**Figures 6A, B** and **S5A**). Specifically, the KEGG complement activation pathway showed robust upregulation of genes affected by SARS-CoV-2 encoding key components of complement components, including *C1q* (*C1qA*, *C1qB*, and *C1qC*), C1 proteases (*C1R* and *C1S*), *CFB*, and complement *C3* (**Figure 6C**). Immunostaining was performed for various complement proteins to validate that the complement cascade is activated in SARS-CoV-2-positive brain tumors. A significant deposition of complement components (C1q and C3)

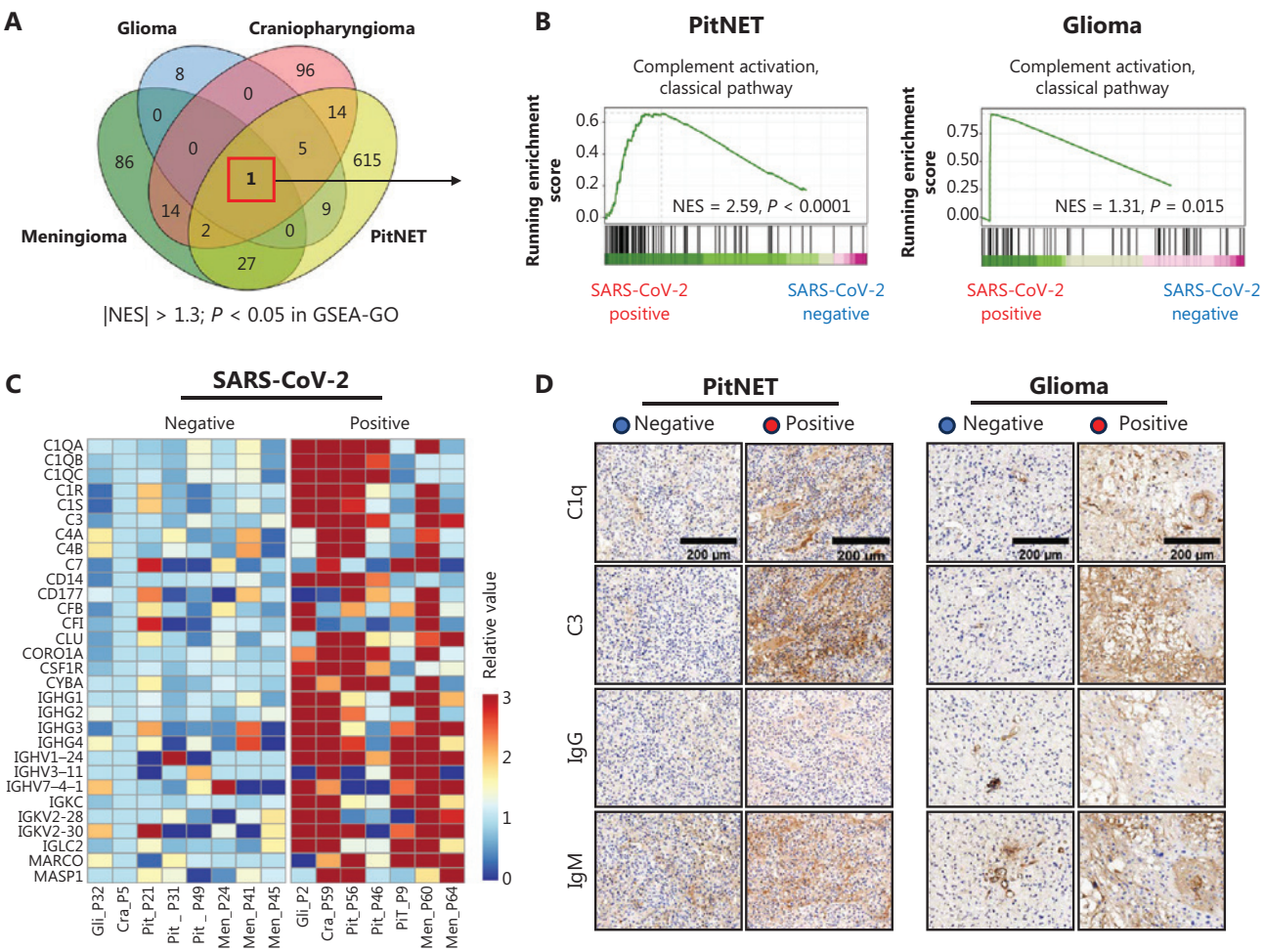


Figure 6 Continued

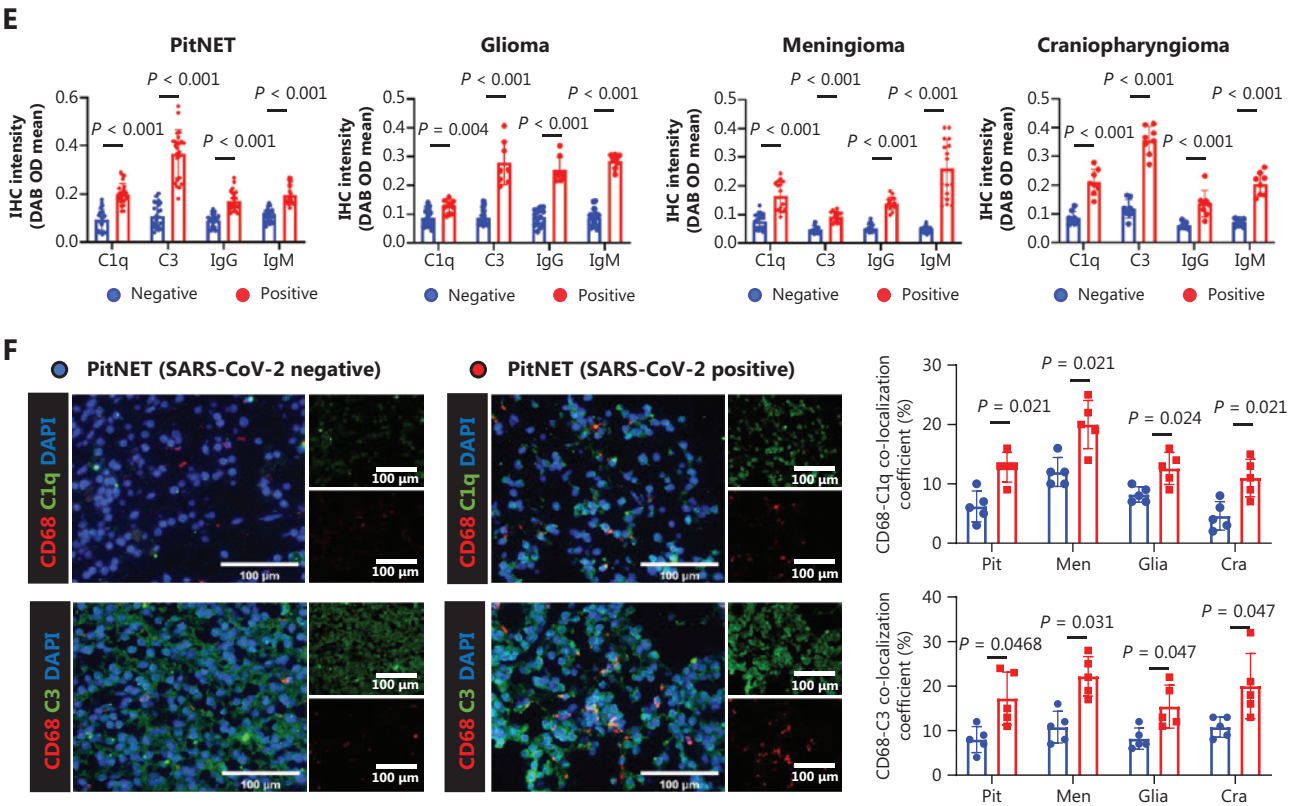


Figure 6 SARS-CoV-2-positive tumors exhibited significant activation of the complement cascade. (A) The Venn diagram shows the overlap of activated pathways related to SARS-CoV-2 infection among glioma, craniopharyngioma, meningioma, and pituitary neuroendocrine tumor samples. (B) Gene set enrichment analysis (GSEA) of complement activation and the classical pathway in SARS-CoV-2-positive pituitary neuroendocrine tumor and glioma samples compared to SARS-CoV-2-negative samples. (C) Heatmap of the relative levels of complement-related gene expression in SARS-CoV-2-positive and -negative brain tumor samples. (D) Representative IHC images of complement components (C1q and C3) and immunoglobulins (IgG and IgM) in pituitary neuroendocrine tumor and glioma tissues that were SARS-CoV-2-negative or -positive. Scale bar: 200 μm. (E) Quantification of the IHC intensity of C1q, C3, IgG, and IgM in SARS-CoV-2-positive and -negative samples from pituitary neuroendocrine tumors, gliomas, meningiomas, and craniopharyngiomas; 5–8 fields/sample were analyzed. (F) Co-localization of C1q/C3 with CD68 in SARS-CoV-2-negative or -positive brain tumors. Tumor sections were double-stained for IF: C1q/C3 (green) and CD68 (macrophage marker, red). Scale bar: 100 μm. Five fields/sample were analyzed. Pit, pituitary neuroendocrine tumors; Men, meningiomas; Glia, gliomas; Cra, craniopharyngiomas. The data represent the mean ± SD; statistical significance was determined by performing the Mann–Whitney *U* test and the adjusted *P* values are reported for multiple testing.

was detected within the tumors, which was correlated with the deposition of IgG and IgM (**Figure 6D**). In contrast, only negligible staining was observed in the brain tumors of the SARS-CoV-2-negative control group (**Figures 6D, E and S5B**). These findings indicated that complement activation is a prominent intracellular response associated with SARS-CoV-2 infection in brain tumors.

Immune cell densities were quantitatively compared between regions with high and low complement deposition (C1q, C3) within the same tumor sections from SARS-CoV-2-positive cases to verify the association between complement activation and immune infiltration. This analysis revealed that areas with intense complement deposition contained a significantly higher density of CD68$^+$ macrophages and CD8$^+$ T cells compared to areas with low complement deposition (**Figure S6A and B**). Furthermore, multiplex immunofluorescence co-staining was performed for complement components (C1q and C3) together with CD68$^+$ macrophages or CD8$^+$ T cells. The results demonstrated greater co-localization of complement components (C1q and C3) with CD68$^+$ macrophages in SARS-CoV-2-positive brain tumors compared to negative tumors (**Figures 6F and S6C**), while CD8$^+$ T cells were notably enriched within areas of complement deposition (**Figure S6D**). These findings suggested that macrophages and CD8$^+$ T cells are key cellular responders to complement activation. Moreover, multiplex immunofluorescence was performed to analyze the co-localization of complement components (C1q and C3) with immune and tumor cells. Complement signals

primarily overlapped with tumor cells, followed by macrophages (~15%), with minimal CD8$^+$ T cell co-localization (**Figure S6C-E**). These results suggested that SARS-CoV-2-infected tumor cells may actively contribute to local complement initiation and amplification, possibly by upregulating and secreting some components (e.g., C3) or serving as sites for deposited complement fragments. Taken together, these findings indicated that local complement production arises from complex interactions between tumor and infiltrating immune cells, particularly macrophages.

Discussion

SARS-CoV-2 infection in brain tumors and the effect on the TIME across nine types of human brain tumors during the BA.5 wave were comprehensively analyzed in the current study. SARS-CoV-2 was detected in several types of brain tumors within the cohort of COVID-19-positive brain tumor patients, including craniopharyngiomas, PitNETs, meningiomas, and gliomas. SARS-CoV-2 infection was shown to be associated with alterations in immune cell infiltration and intratumor innate immune signaling activation, especially the complement cascade.

The current study provided histopathologic evidence of SARS-CoV-2 infection in multiple brain tumor types from COVID-19 patients. Viral RNA was identified in 8 of 72 (11%) tumor samples with no detection in adjacent paracarcinoma tissues. In addition, viral RNAs and/or proteins were identified in four types of brain tumors (craniopharyngiomas, PitNETs, meningiomas, and gliomas), supporting the notion that SARS-CoV-2 has recently undergone active replication or at least completed the processes of viral entry and uncoating. These findings are similar to previous reports of SARS-CoV-2 detection in the cerebral cortex and pituitary gland of COVID-19 patients[5,18]. However, the susceptibility of gliomas to SARS-CoV-2 infection remains poorly characterized with current evidence limited to case reports[19] and *in vitro* monolayer systems[20,21]. Disruption of the BBB in brain tumors, coupled with a immunosuppressive tumor microenvironment[7,8], may facilitate viral neuro-invasion through peripheral nerves and bloodstream routes[6]. Immunohistochemical localization demonstrated viral infection in tumor and endothelial cells within the brain tumors. Expression of the classical SARS-CoV-2 receptor, ACE2, and the key co-factor, TMPRSS2 was absent or very low in tumor cells among the examined brain tumor tissues. However, marked high expression of the alternative receptors, neuropilin-1 (NRP1) and CD147 (BSG), was noted. SARS-CoV-2 infection of brain tumor cells may not rely on the ACE2-TMPRSS2 axis but could be mediated through mechanisms, such as endocytosis *via* the NRP1 and/or CD147 pathways. Unlike endothelial cells and astrocytes, which may express elevated levels of ACE2[22,23], the data herein indicated that brain tumor cells exhibit a distinct "ACE2$^-$/TMPRSS2$^-$, NRP1$^+$/CD147$^+$" phenotype. This finding suggests that the virus may utilize fundamentally different "molecular keys" to invade different brain cell types. In addition, the results of the molecular analysis revealed higher expression of SARS-CoV-2 entry mediators, particularly NRP1, in human brain tumor tissues than normal brain tissue[17,24], which further suggests a potential tropism of SARS-CoV-2 for infecting brain tumor cells. Thus, the findings herein indicated that brain tumors might be vulnerable to SARS-CoV-2 infection, highlighting the need for further investigation into the mechanisms underlying viral tropism and the effect on tumor biology and progression.

Greater macrophage infiltration was demonstrated in SARS-CoV-2-positive brain tumors than negative controls. Macrophages are the most abundant immune cells in the brain tumor microenvironment are are critical for viral recognition and bridging innate and adaptive immunity[25]. CD8$^+$ or IFN-γ^+ CD8$^+$ T cells were more abundant in SARS-CoV-2-positive brain tumors than negative controls. Moreover, CD8$^+$ T cell infiltration exhibited a correlative trend with viral load. These CD8$^+$ T lymphocytes are essential for the adaptive immune response against viral infections and the presence in brain tumors suggests activated antitumor immunity[26]. This finding strongly supports a "dose-dependent" relationship in the strength of the adaptive anti-viral immune response, suggesting that SARS-CoV-2 infection directly or indirectly drives the recruitment and/or expansion of tumor-specific or virus-specific CD8$^+$ T cells. SARS-CoV-2 infection might disrupt the immunosuppressive environment of brain tumors, create a more immunogenic microenvironment, and thereby improve the effectiveness of immunotherapy. This finding is consistent with studies demonstrating differences in the immune microenvironments of lung cancer patients with and without SARS-CoV-2 infection[27]. Moreover, various case studies have indicated that SARS-CoV-2 infection may have oncolytic effects on individuals with blood cancer, metastatic colon cancer, and clear cell renal cell carcinoma[28-32]. If SARS-CoV-2 infection can trigger a lasting systemic anti-tumor immunity, a positive impact on delaying tumor progression or improving patient outcomes may occur. However, the overall effect of SARS-CoV-2 infection on brain tumors likely depends on multiple factors, including tumor type, genetic background, patient immune status, as well as the viral infection dose and timing.

An unbiased and comprehensive transcriptome analysis was performed to clarify the mechanisms underlying the changes in the TIME associated with SARS-CoV-2 infection. The results revealed that SARS-CoV-2 infection leads to substantial transcriptional changes in several key biological processes, including complement activation, phagocytosis, cell cycle regulation, and oncogenic pathways. Innate immune responses were significantly enriched in SARS-CoV-2-infected brain tumors.

The GSEA and immunohistochemical data showed that the classical complement pathway is strongly activated in SARS-CoV-2-positive tumors with key components, such as C1q and C3, being upregulated and deposited in tumor tissues. This coordinated multi-pathway response is more consistent with an integrated host defense against SARS-CoV-2 than non-specific, dysregulated tissue inflammation. The complement cascade is an essential component of the innate immune system that orchestrates the release of inflammatory mediators, phagocytic responses, and cell lysis[33,34]. We consider that activation of the complement system is the core bridge connecting viral infection and T-cell responses. Immune cell densities between regions with high and low complement deposition (C1q and C3) were quantitatively compared. The results showed greater co-localization of complement components with $CD68^+$ macrophages and $CD8^+$ T cells. Recent studies have shown that activation of the complement system has a role in the pathogenesis of severe SARS-CoV-2 infection[13,35,36]. Complement activation products (C5a and C3a) are powerful chemokines that directly chemoattract T cells, including $CD8^+$ T cells, to inflammatory sites[37]. In addition, these complement components, such as C1q, and subsequently deposited immunoglobulins (IgG/IgM) can form antigen-antibody complexes. The latter can serve as strong immune stimulatory signals through the bridging of antigen-presenting cells, such as macrophages, indirectly promote the activation and clonal proliferation of $CD8^+$ T cells, thereby exerting antiviral and even potential antitumor effects.

The IFA analysis herein revealed that complement components (C1q/C3) are predominantly co-localized with tumor cells (~80%), implicating virus-infected tumor cells as a major source and site of complement deposition. Macrophages accounted for most of the remaining signal (~20%), suggesting a role as responders and potential local producers. The activation is likely initiated by pre-existing SARS-CoV-2-specific antibodies forming immune complexes with local viral antigens *via* the classical pathway, which is then amplified by the tumor microenvironment. This localized complement response may function as an endogenous immune adjuvant within the infected tumors. Activating the complement system locally in tumors by delivery of complement component agonists or nanomaterials could replicate the immune activation caused by viral infections, counteract the immunosuppressive environment of brain tumors, and enhance the effectiveness of current immunotherapies, such as immune checkpoint inhibitors. In addition, there is a potential risk of abnormal complement-driven immune activation in the brain among COVID-19 patients with brain tumors. Monitoring markers of complement activity could help identify those patients who might benefit from managing CNS complications.

The current study had some limitations. First, RT-qPCR primers targeted the conserved regions of *N* and *ORF1ab*; it is impossible to determine whether the viral RNA is derived from BA.5 or earlier variants based solely on this data. Second, we were unable to systematically and completely obtain the SARS-CoV-2 infection history of all 72 patients prior to the BA.5 infection event. Third, SARS-CoV-2 infection was associated with alterations in the brain TIME immune microenvironment but evidence of a causal relationship is lacking. Finally, it remains unclear whether the immune infiltration resulting from viral infection specifically targeted the virus, tumor cells, or both. Further studies are needed to investigate the tumor progression and long-term effects of SARS-CoV-2 infection.

Notably, despite a limited sample size, a uniform viral background was noted in the BA.5 wave and consistently detected SARS-CoV-2 with complement activation in multiple brain tumor types. This finding suggests that infection-triggered immune remodeling is a common feature of these cancers. The data support a model wherein SARS-CoV-2 infection profoundly remodels the TIME, potentially creating a state that is permissive for anti-tumor immunity in addition to simply recruiting virus-specific T cells, as follows: (1) The transcriptomic analysis revealed that SARS-CoV-2-positive tumors are characterized by a significant enrichment of pathways related to "interferon-gamma response," "immune cell infiltration," and "phagocytosis" coupled with the activation of multiple innate antiviral immune pathways. This signature indicates a broad shift from an immunosuppressive state to an immunologically active state, aligning with an effector anti-tumor phenotype. (2) The robust complement cascade activation serves as a key mechanistic link. Complement cleavage products are potent chemo-attractants and inflammatory mediators that can non-specifically recruit and activate various immune cells, including macrophages and T cells, and enhance antigen presentation. Thus, the virus-triggered complement response likely acts as an immunologic adjuvant, reshaping the immune microenvironment. These findings highlighted the role of SARS-CoV-2 in modulating the tumor immune landscape and offer insights into the complex interaction between viral infections and tumor progression.

Conclusions

Overall, the current study provides the first human-tissue evidence that SARS-CoV-2 can infect various primary brain tumors. Importantly, infection is associated with significant remodeling of the local TIME, characterized by robust complement system activation, increased infiltration of immune effector cells, such as $CD8^+$ T cells, and downregulation of specific oncogenic pathways. These findings suggested that SARS-CoV-2 infection may transiently reverse the immunosuppressive state of brain tumors by triggering a complement-driven innate immune response. This work offers a novel perspective on virus-tumor-immune interactions and highlights potential avenues for immunomodulatory therapeutic strategies.

Acknowledgments

We gratefully acknowledge the staff at the Precision Medicine Research Institute of the First Affiliated Hospital of Sun Yat-sen University for support and facilitation of the study.

Grant support

This study was supported by the National Natural Science Foundation of China (Grant Nos. 82372624, 82573778, and 82504174), the Guangdong Basic and Applied Basic Research Foundation (Grant No. 2024A1515013102), the Guangdong Pearl River Talent Program (Grant No. 2023ZT10Y094), the China Postdoctoral Science Foundation (Grant No. 2022M723588), the Medical Scientific Research Foundation of Guangdong Province (Grant No. A2023439), Science and Technology Empowering Inner Mongolia Major Special Project of Inner Mongolia Autonomous Region (Grant No. 2022-KJXM-ZCQ-11), and the Guangdong Basic and Applied Basic Research Foundation (Grant No. 2023A1515110422).

Conflict of interest statement

No potential conflicts of interest are disclosed.

Author contributions

Conceived and designed the analysis: Weikang Chen, Xiaobing Jiang, Xiaoxing Li.
Collected the data: Haojie Bai, Maoling Tian, Lei Zhou, Wange Lu.
Contributed data or analysis tools: Yanxia Huang, Depei Li, Linyi Liu.
Performed the analysis: Weikang Chen, Haojie Bai, Yanxia Huang, Luyao Wu, Wei Li.
Wrote the paper: Weikang Chen, Haojie Bai, Xiaobing Jiang.

Data availability statement

The data generated in this study are available upon request from the corresponding author.

References

1. Hensley MK, Markantone D, Prescott HC. Neurologic manifestations and complications of COVID-19. Annu Rev Med. 2022; 73: 113-27.
2. Helms J, Kremer S, Merdji H, Clere-Jehl R, Schenck M, Kummerlen C, et al. Neurologic features in severe SARS-CoV-2 infection. N Engl J Med. 2020; 382: 2268-70.
3. Alwan NA. Lessons from Long COVID: working with patients to design better research. Nat Rev Immunol. 2022; 22: 201-2.
4. Al-Aly Z, Xie Y, Bowe B. High-dimensional characterization of post-acute sequelae of COVID-19. Nature. 2021; 594: 259-64.
5. Stein SR, Ramelli SC, Grazioli A, Chung JY, Singh M, Yinda CK, et al. SARS-CoV-2 infection and persistence in the human body and brain at autopsy. Nature. 2022; 612: 758-63.
6. Bauer L, Laksono BM, de Vrij FMS, Kushner SA, Harschnitz O, van Riel D. The neuroinvasiveness, neurotropism, and neurovirulence of SARS-CoV-2. Trends Neurosci. 2022; 45: 358-68.
7. Arvanitis CD, Ferraro GB, Jain RK. The blood-brain barrier and blood-tumour barrier in brain tumours and metastases. Nat Rev Cancer. 2020; 20: 26-41.
8. Quail DF, Joyce JA. The microenvironmental landscape of brain tumors. Cancer Cell. 2017; 31: 326-41.
9. Yaniv D, Mattson B, Talbot S, Gleber-Netto FO, Amit M. Targeting the peripheral neural-tumour microenvironment for cancer therapy. Nat Rev Drug Discov. 2024; 23: 780-96.
10. Gajewski TF, Schreiber H, Fu YX. Innate and adaptive immune cells in the tumor microenvironment. Nat Immunol. 2013; 14: 1014-22.
11. Sampson JH, Gunn MD, Fecci PE, Ashley DM. Brain immunology and immunotherapy in brain tumours. Nat Rev Cancer. 2020; 20: 12-25.
12. Diamond MS, Kanneganti TD. Innate immunity: the first line of defense against SARS-CoV-2. Nat Immunol. 2022; 23: 165-76.
13. Yan B, Freiwald T, Chauss D, Wang L, West E, Mirabelli C, et al. SARS-CoV-2 drives JAK1/2-dependent local complement hyperactivation. Sci Immunol. 2021; 6: eabg0833.
14. Afzali B, Noris M, Lambrecht BN, Kemper C. The state of complement in COVID-19. Nat Rev Immunol. 2022; 22: 77-84.
15. Meri S, Magrini E, Mantovani A, Garlanda C. The Yin Yang of complement and cancer. Cancer Immunol Res. 2023; 11: 1578-88.
16. Roumenina LT, Daugan MV, Petitprez F, Sautès-Fridman C, Fridman WH. Context-dependent roles of complement in cancer. Nat Rev Cancer. 2019; 19: 698-715.
17. Chen W, Jiang X, Liang W, Bai H, Xu M, Liu Z, et al. SARS-CoV-2 Omicron variants show attenuated neurovirulence compared with the wild-type strain in elderly human brain spheroids. Research (Wash D C). 2024; 7: 0376.
18. Poma AM, Proietti A, Macerola E, Bonuccelli D, Conti M, Salvetti A, et al. Suppression of pituitary hormone genes in subjects who died from COVID-19 independently of virus detection in the gland. J Clin Endocrinol Metab. 2022; 107: 2243-53.
19. Lei J, Liu Y, Xie T, Yao G, Wang G, Diao B, et al. Evidence for residual SARS-CoV-2 in glioblastoma tissue of a convalescent patient. Neuroreport. 2021; 32: 771-5.
20. Chu H, Chan JF, Yuen TT, Shuai H, Yuan S, Wang Y, et al. Comparative tropism, replication kinetics, and cell damage profiling of SARS-CoV-2 and SARS-CoV with implications for clinical manifestations, transmissibility, and laboratory studies of COVID-19: an observational study. Lancet Microbe. 2020; 1: e14-23.

21. Bielarz V, Willemart K, Avalosse N, De Swert K, Lotfi R, Lejeune N, et al. Susceptibility of neuroblastoma and glioblastoma cell lines to SARS-CoV-2 infection. Brain Res. 2021; 1758: 147344.
22. Coelho SVA, Souza GLE, Bezerra BB, Lima LR, Correa IA, de Almeida DV, et al. SARS-Cov-2 replication in a blood-brain barrier model established with human brain microvascular endothelial cells induces permeability and disables ACE2-dependent regulation of bradykinin B1 receptor. Int J Mol Sci. 2025; 26: 5540.
23. Chen R, Wang K, Yu J, Howard D, French L, Chen Z, et al. The spatial and cell-type distribution of SARS-CoV-2 receptor ACE2 in the human and mouse brains. Front Neurol. 2020; 11: 573095.
24. Suarez-Meade P, Watanabe F, Ruiz-Garcia H, Rafferty SB, Moniz-Garcia D, Schiapparelli PV, et al. SARS-CoV2 entry factors are expressed in primary human glioblastoma and recapitulated in cerebral organoid models. J Neurooncol. 2023; 161: 67-76.
25. Sang Y, Miller LC, Blecha F. Macrophage polarization in virus-host interactions. J Clin Cell Immunol. 2015; 6: 311.
26. Schmidt ME, Varga SM. The CD8 T cell response to respiratory virus infections. Front Immunol. 2018; 9: 678.
27. Malkani N, Rashid MU. SARS-COV-2 infection and lung tumor microenvironment. Mol Biol Rep. 2021; 48: 1925-34.
28. Pasin F, Mascalchi Calveri M, Calabrese A, Pizzarelli G, Bongiovanni I, Andreoli M, et al. Oncolytic effect of SARS-CoV2 in a patient with NK lymphoma. Acta Biomed. 2020; 91: e2020047.
29. Kandeel EZ, Refaat L, Abdel-Fatah R, Samra M, Bayoumi A, Abdellateif MS, et al. Could COVID-19 induce remission of acute leukemia? Hematology. 2021; 26: 870-3.
30. Ottaiano A, Scala S, D'Alterio C, Trotta A, Bello A, Rea G, et al. Unexpected tumor reduction in metastatic colorectal cancer patients during SARS-Cov-2 infection. Ther Adv Med Oncol. 2021; 13: 17588359211011455.
31. Choong OK, Jakobsson R, Bergdahl AG, Brunet S, Kärmander A, Waldenström J, et al. SARS-CoV-2 replicates and displays oncolytic properties in clear cell and papillary renal cell carcinoma. PLoS One. 2023; 18: e0279578.
32. Chen X, Jiang B, Gu Y, Yue Z, Liu Y, Lei Z, et al. SARS-CoV-2 nucleocapsid protein interaction with YBX1 displays oncolytic properties through PKM mRNA destabilization. Mol Cancer. 2024; 23: 248.
33. Ricklin D, Hajishengallis G, Yang K, Lambris JD. Complement: a key system for immune surveillance and homeostasis. Nat Immunol. 2010; 11: 785-97.
34. Schartz ND, Tenner AJ. The good, the bad, and the opportunities of the complement system in neurodegenerative disease. J Neuroinflammation. 2020; 17: 354.
35. Ma L, Sahu SK, Cano M, Kuppuswamy V, Bajwa J, McPhatter J, et al. Increased complement activation is a distinctive feature of severe SARS-CoV-2 infection. Sci Immunol. 2021; 6: eabh2259.
36. Holter JC, Pischke SE, de Boer E, Lind A, Jenum S, Holten AR, et al. Systemic complement activation is associated with respiratory failure in COVID-19 hospitalized patients. Proc Natl Acad Sci U S A. 2020; 117: 25018-25.
37. Guo RF, Ward PA. Role of C5a in inflammatory responses. Annu Rev Immunol. 2005; 23: 821-52.

Cite this article as: Chen W, Bai H, Tian M, Huang Y, Li D, Wu L, et al. SARS-CoV-2 infection in brain tumors and the association with alterations in the tumor immune microenvironment. Cancer Biol Med. 2026; 23: 769-784. doi: 10.20892/j.issn.2095-3941.2025.0468